CHALMERS
UNIVERSITY OF TECHNOLOGY

Upgrade and benchmark of quasi-linear transport model EDWM

Physics of Plasmas

Upgrade and benchmark of quasi-linear transport model EDWM

Cite as: Phys. Plasmas **29**, 112305 (2022); https://doi.org/10.1063/5.0119515
Submitted: 09 August 2022 • Accepted: 19 October 2022 • Published Online: 08 November 2022

E. Fransson, H. Nordman, P. Strand, et al.

Physics of Plasmas ARTICLE scitation.org/journal/php

Upgrade and benchmark of quasi-linear transport model EDWM

Cite as: Phys. Plasmas **29**, 112305 (2022); doi: 10.1063/5.0119515
Submitted: 9 August 2022 · Accepted: 19 October 2022 ·
Published Online: 8 November 2022

E. Fransson,[a] H. Nordman,[b] P. Strand,[c] and JET Contributors[d]

AFFILIATIONS

Space, Earth and Environment, Chalmers University of Technology, Gothenburg 412 96, Sweden

[a]Author to whom correspondence should be addressed: emil.fransson@chalmers.se
[b]E-mail: hans.nordman@chalmers.se
[c]E-mail: par.strand@chalmers.se
[d]See Joffrin *et al.* (2019) (https://doi.org/10.1088/1741-4326/ab2276) for the JET Contributors.

ABSTRACT

The verification of a new saturation rule applied to the quasi-linear fluid model EDWM (extended drift wave model) and the calibration of several other features are presented. As one of the computationally fastest first-principle-based core transport models, EDWM can include an arbitrary number of ions and charge states. This feature is especially important for experimental devices with plasma-facing components made of heavy elements, such as the upcoming ITER device. As a quasi-linear model, EDWM solves a linear dispersion relation to obtain the instabilities driving the turbulence and combines the linear description with an estimation of the saturation level of the electrostatic potential to determine the fluxes. A new saturation rule at the characteristic length combined with a spectral filter for the poloidal wavenumber dependency is developed. The shape of the filter has been fitted against the poloidal wavenumber dependency of the electrostatic potential from non-linear gyrokinetic simulations. Additionally, EDWM's collision frequency and safety factor dependencies, as well as the electron heat flux level, have been calibrated against gyrokinetic and gyrofluid results. Finally, the saturation level has been normalized against non-linear gyrokinetic simulations and later validated against experimental measured fluxes from 12 discharges at JET.

I. INTRODUCTION

Integrated modeling of fusion plasmas plays a key role for interpretation, prediction, and optimizing of present-day experiments and is expected to be instrumental for the design of a demonstration fusion power plant (DEMO). With current computing resources, it is not possible to make complete non-linear gyrokinetic simulations of a whole fusion plasma. For this reason, reduced models of different processes, including turbulent transport, heating, and current drive sources, have to be integrated to build up a complete fusion plasma simulation.[1–4] Because the performance of a tokamak fusion plasma is largely determined by turbulent transport, it is crucial to model this process accurately. The simulations with the greatest physics fidelity that are currently employed to analyze turbulent transport in tokamak plasma are based on gyrokinetic theory. Here, the fast time scales associated with the Larmor gyration of particles have been averaged over, which is motivated by the fact that the transport processes typically take place on much slower timescales. Despite the simplification offered by gyrokinetic theory, the computing cost associated with running gyrokinetic codes is still prohibitive for routine analysis of tokamak discharges. Consequently, models with additional simplifications have been developed, mainly based on the quasi-linear approach which we define as using a linear dispersion relation and linear relations between the perturbations in combination with a model for the saturation of the fields. Based on this approach, a number of models have been developed, including QuaLiKiz,[5] Trapped-Gyro-Landau-Fluid (TGLF),[6] fluid models like Weiland,[7] and extended drift wave model (EDWM).[8] These models are currently being used within a number of integrated modeling frameworks, especially the European Transport Solver (ETS),[1,2] ASTRA,[3] and JINTRAC.[4] Recently, the quasi-linear models have been verified against non-linear gyrokinetic simulations[9,10] and validated against experimental measurements.[11–20] However, the physics fidelity of the reduced models based on quasi-linear theory mentioned above is not up to the standard of gyrokinetic codes in all areas, especially not when it comes to non-linear effects, for example, zonal flows. The question therefore arises if one can use output from gyrokinetic codes to calibrate corrections to the

quasi-linear models such that they better reproduce key features of the physics where these models are known to have deficiencies. This has proved to be possible, and enhanced versions of the quasi-linear models have been presented as following advances in non-linear gyrokinetic simulations.

The purpose of the present paper is to explore corrections that can be applied to EDWM such that it better reproduces the main trends found in gyrokinetic simulations in key areas. Lately, this has become a common feature when developing quasi-linear models and they have benefited from comparison with non-linear simulations, such as the latest updates of TGLF.[10,21] Improvements to the EDWM model are valuable because the computation time it requires is substantially shorter than for most other quasi-linear models owing to the simplifications afforded by not directly accounting for certain effects, such as finite Larmor radius (FLR) effects and Landau resonances (some of the associated features are nevertheless taken into account approximately in EDWM). Consequently, EDWM is particularly suited for routine simulations of fusion plasmas. EDWM also excels in terms of accounting for impurity ions, and it can handle an arbitrary number of such ion species and any charge state. This is particularly important for the analysis of devices with plasma-facing components made from heavy elements (mainly tungsten), including JET, ASDEX-Upgrade, ITER, and a future DEMO.

In this work, we benefit from published databases of gyrokinetic simulations[22,23] to introduce and calibrate enhancements/corrections to EDWM. In particular, five areas where enhancements/corrections can be applied are studied: (I) a new poloidal wavenumber filter; (II) a correction factor for the role of collisionality; (III) an adjustment of the balance between the electron and ion heat fluxes; (IV) a correction factor for the scaling of the turbulent transport with the safety factor q; and (V) a new rule for the saturation of the fluctuation level (mainly to adapt to the updated poloidal wavenumber filter).

A review of key theoretical aspects of turbulent transport modeling needed as a background to the enhancements and corrections discussed in this paper is given in Sec. II. Furthermore, the databases of gyrokinetic simulations and results from JET experiments used for benchmarking in this paper are briefly described in Sec. III. The five different improvements implemented in EDWM are discussed in Sec. IV:

(I) In the original version of EDWM, five poloidal wavenumbers, centered around the wavenumber giving the greatest turbulent transport for a Deuterium plasma, are used. However, a distribution of just five wavenumbers has been found insufficient to reflect the fact that there are several instabilities driving turbulence with peak effect at different wavenumbers.[24] For this reason, a new filter with eleven mode numbers has been implemented in EDWM, and the determination of its form with the aid of results from GENE simulations is discussed in Sec. IV A.

(II) The dependence of the turbulent transport on the plasma collisionality in EDWM reproduces that of gyrokinetic simulations well at low and high collisionality. However, the trend at intermediate collisionality is not well captured in the basic version of EDWM. In Sec. IV B, a correction factor for the collisionality is therefore explored. In particular, it aims to reproduce the zero flux peaking factor found in gyrokinetic and gyrofluid simulations (i.e., the peaking of density and temperature profiles where the convective transport term balances the diffusive one), which is very sensitive to the collisionality.[25]

(III) In the original EDWM model, the balance between heat transport in the electron and ion transport channels is too skewed toward the latter when compared to gyrokinetic simulations. In order to redress the balance, a correction factor is invoked in Sec. IV C and its value is determined with the aid of benchmarking against GENE simulations.

(IV) There is a spectral shift of the turbulence as the safety factor, q, changes in non-linear gyrokinetic simulations, which is not captured in the original EDWM. In order to better reproduce the spectral change found in gyrokinetic simulations, a power law correction with q to EDWM is investigated in Sec. IV D. The correction is obtained by comparison with a database of published results from the GYRO code.[23]

(V) With the enhancement and corrections discussed above, especially the new poloidal wavenumber filter, it is necessary to update the rule for the saturation level of the turbulence. The rational behind the new rule is discussed in Sec. II A, and benchmarking with GENE results to determine the level of fluctuations is provided in Sec. IV E.

II. EDWM MODEL

EDWM is based on the Weiland model created at Chalmers University of Technology in the 90s,[7] and it is applicable for turbulent transport in conventional tokamaks. It is a fluid model, which was initially developed only for the ion temperature gradient (ITG) mode[26] and subsequently expanded to include the trapped electron mode.[27] EDWM only considers instabilities at ion scales and does not include instabilities at smaller scales, such as the electron temperature gradient (ETG) mode. The ITG mode is usually responsible for the majority of the turbulent fluxes in today's experimental devices and is driven by the gradient in the ion temperature. Both the ITG and TEM are at ion scales, with the ITG mode being the most unstable around $0.3\ k_y\rho_{s,H}$ and the TEM at slightly smaller scales. Here, k_y is the poloidal wavenumber and it is normalized with $\rho_{s,H} = c_{s,H}/\Omega_{c,H}$, where $c_{s,H}$ is the ion sound speed and $\Omega_{c,H}$ is the cyclotron frequency both taken for hydrogen. The TEM is associated with a fraction of the electrons, which are trapped on the bad curvature side of the torus. The free (passing) electrons are described as Boltzmann distributed with an electromagnetic correction and EDWM considers all trapped electrons as deeply trapped. The Weiland model only used a single poloidal wavenumber to calculate the flux, at the typical length scale for the ITG mode for Deuterium. However, this single poloidal wavenumber approach is problematic for different isotopes, as the typical physical length scale of the ITG mode depends on the mass of the isotope. Hence, EDWM was developed with the purpose to be able to handle different isotopes and mixed plasma as one as its most important features. This was achieved by modeling the fluxes for a spectrum of poloidal wavenumbers.[8] EDWM can handle an arbitrary number of ions and all their possible charge states.[28] Higher order finite Larmor radius effects have been added to the later version of EDWM. The derivation of the multi-fluid model starts with the Braginskii equations coupled to Maxwell's equations. It is electromagnetic, and as a consequence, the free electrons are not Boltzmann distributed due to the

correction from the vector potential parallel with the magnetic field. Another electromagnetic effect is the stabilization of the ion temperature gradient (ITG) mode, which usually is the dominant turbulent instability in current experimental devices. EDWM uses a toroidal slab geometry, and the E × B-shearing rate is taken into account as a reduction in the linear growth rate in the Hahm–Burrell formalism.[29] As EDWM uses an eigenvalue solver, all unstable modes not just the most unstable, account for the total flux.

A. Quasi-linear theory

As EDWM is a quasi-linear model, it solves a linear dispersion relation; hence, it does not get the saturated quantities directly as in the non-linear case. Quasi-linear theory connects the linear growth rates, real frequencies, and other plasma parameters to the saturated quantities, such as the electrostatic potential. The turbulent fluxes in the plasma are caused by the interaction between the electrostatic potential and the perturbed quantities (density, temperature). The turbulent fluxes are given by the linear phase difference between the perturbed quantities and the E × B drift

$$\begin{aligned}\Gamma_i &= \langle \delta n_i v_{ExB} \rangle, \\ Q_i &= \langle \delta T_i v_{ExB} \rangle\end{aligned} \tag{1}$$

and the brackets denote flux surface and time averages. An additional contribution to the fluxes exists, from the magnetic flutter, which originates from the perturbation in the vector potential parallel with the magnetic field. However, this contribution is not included in EDWM as it is usually small in comparison with the E × B-part; however, under certain circumstances, it can be appreciable.[30] The expression for the E × B contribution to the fluxes can be further developed,[31] here for the particle transport

$$\Gamma = n_0 \rho_s c_s 2 \sum_1^\infty k_y \underbrace{\frac{\delta \hat{n}_{k,r} \hat{\phi}_{k,i} - \delta \hat{n}_{k,i} \hat{\phi}_{k,r}}{\hat{\phi}_k \hat{\phi}_k^*}}_{\text{Phase shift, independent of sat. level}} \underbrace{|\hat{\phi}_k|^2}_{\text{Saturation level}}. \tag{2}$$

Here, the i and r represent the imaginary and real part and $\hat{\phi}$ is the normalized electrostatic potential. n_0 is the background density, ρ_s is the gyro-radius, c_s is the plasma sound speed, and k_y represents the poloidal wavenumber. We use a slab geometry with x in the radial direction and y in the poloidal direction. The sum is over all wavenumbers but only a limited part of spectrum at low wavenumber has a significant contribution to the fluxes. The last part of Eq. (2) describes the saturation level, also called quasi-linear intensity, which is discussed later in detail. The fraction describes the phase difference between the electrostatic potential and the perturbed quantity. Interestingly, we do not get any fluxes if they are in phase, as in the case for perfectly Boltzmann-distributed electrons. It is clear that it is essential that the linear phase differences calculated by EDWM have similar values as the non-linear counterpart. This is one of the two main criteria for quasi-linear theory. These criteria have been extensively studied by comparing non-linear and quasi-linear simulations and generally hold.[32,33] Second, the random walk assumption needs to hold and a condition for this is that the Kubo number[34] needs to smaller than 1. The Kubo number represents the ratio between the decorrelation time for the electrostatic potential and the turbulent eddy turn over time. The Kubo number has been calculated for several plasmas in different machines and different turbulence regimes, and it has consistently been lower than 1.[35,36] Hence, it has been that for typical plasma parameters, the random walk assumption is valid.

The connection between the electrostatic potential and the linear growth rate is expressed by the mixing length assumption, which will result in an expression for the saturation level, the last part in Eq. (2). It originates from that the convective E × B non-linearity in the energy equation is balanced by the linear growth rate

$$\gamma \delta T_j \sim \boldsymbol{v}_{ExB} \cdot \nabla \delta T_j. \tag{3}$$

In the original EDWM,[8] a range of wavenumbers is used and an approximate saturation level is derived from Eq. (3) at each length scale. This yields the usual mixing length assumption, which may be written as

$$\frac{e\phi(k_y)}{T_e} = \hat{\phi}(k_y) = \frac{\gamma}{k_x k_y} \frac{1}{\rho_s c_s}. \tag{4}$$

The resulting spectrum given by Eq. (4) overestimates the fluxes at low wavenumbers, which is shown in Sec. IV A. Our aim is to improve the saturation model by introducing a spectral filter. This will be obtained by comparisons with gyrokinetic simulations in Sec. IV A 1. The resulting filter is then combined with the saturation model of Eq. (4), but with the wavenumbers taken at a characteristic length scale, described by $k_{x,a}$ and $k_{y,a}$, where the turbulent transport is maximum. The saturation is thus given by

$$\frac{e\phi_a}{T_e} = \hat{\phi}_a = \frac{\gamma}{k_{x,a} k_{y,a}} \frac{1}{\rho_s c_s}. \tag{5}$$

An improved treatment of the mixing length can be found by looking more thoroughly at Eq. (3). The gradients in the E × B-drift velocity and of the perturbed quantities are easily calculated if we express them and the electrostatic potential as Fourier series. Here, for a slab geometry with x as the radial coordinate and y the poloidal

$$\begin{aligned}\delta T(x,y) &= \sum_{k_{x1},k_{y1}} \delta T_{k_{x1},k_{y1}} e^{ik_{x1}x} e^{ik_{y1}y}, \\ \phi(x,y) &= \sum_{k_{x2},k_{y2}} \phi_{k_{x2},k_{y2}} e^{ik_{x2}x} e^{ik_{y2}y},\end{aligned} \tag{6}$$

where $\delta T_{k_{x1},k_{y1}}$ and $\phi_{k_{x2},k_{y2}}$ are Fourier coefficients and are independent of the spatial coordinates. The RHS of Eq. (3) becomes

$$\sum_{\substack{k_{x1},k_{y1} \\ k_{x2},k_{y2}}} \left(\frac{k_{x1}k_{y2}}{B} - \frac{k_{x2}k_{y1}}{B} \right) \delta T_{k_{x1},k_{y1}} \phi_{k_{x2},k_{y2}} e^{ix(k_{x1}+k_{x2})} e^{iy(k_{y1}+k_{y2})}. \tag{7}$$

We notice that we get two similar terms, one from the radial direction and one from the poloidal from the inner product in Eq. (3). We can remove the spatial dependency by multiplying with test functions $e^{ik_{x3}}$ and $e^{ik_{y3}}$, thereafter integrating over the slab geometry. We end up with an expression

$$\gamma_{k_{x3},k_{y3}} \delta T_{k_{x3},k_{y3}} \sim \sum_{k_{x2},k_{y2}} \left(\frac{k_{x3}k_{y2} - k_{x2}k_{y3}}{B} \right) \delta T_{k_{x3}-k_{x2},k_{y3}-k_{y2}} \phi_{k_{x2},k_{y2}}. \tag{8}$$

This equation expresses the balance between the linear growth and the non-linear mode coupling. The linear term for each poloidal

wavenumber is balanced by a sum over wavenumber for the non-linear interaction term. This summation is referred to as the drift wave mixing. The expression for the mixing length, Eq. (5), conveys the same physics as Eq. (8), although in a more rudimentary version. As the mode-coupling in Eq. (8) cannot properly be represented in a quasi-linear model, and as Eq. (5) is only valid at the characteristic length, we introduce the following saturation rule for the new version of EDWM. We propose that the saturation level is taken at the correlation length scale and all dependence of the poloidal wavenumber is contained in a filter f, representing the mode-coupling. We write the electrostatic potential as

$$|\hat{\phi}|^2(k_y\rho_{s,H}) = \frac{4\gamma_a^2}{\omega_{Dea}R^2k_a^2} f^2(k_y\rho_{s,H}). \tag{9}$$

Here, it is normalized with ω_{De}, the electron diamagnetic drift frequency. From here on out, we will use k_y as substitute for $k_y\rho_{s,H}$ for brevity. The fraction is calculated at the characteristic length, and the function f determines the spectral shape. The implementation and shape of the filter is discussed in Sec. IV A.

III. GYROKINETIC BENCHMARK

We have compared our EDWM simulations with three sets of data to introduce corrections to the model: first, 17 gyrokinetic simulations with GENE,[22] second data from the GA GYRO database,[23] and finally from four collisionality scans at JET. The GENE simulations have been used to create a new spectral filter by determining the characteristic length for the turbulence. The ratio between different transport channels in these simulations have been used to approximate their counterpart in EDWM. The GA GYRO database includes safety factor scans, which have been used to determine EDWM dependence on the safety factor. Finally, the data from the JET collisionality scans have been used to validate the fluxes of the new version of EDWM.

A. GENE simulations

The comparison with EDWM has primarily been done against 17 GENE simulations. The GENE model uses a Eulerian δf method to solve the non-linear gyrokinetic Vlasov equation. We have used the linearized Landau–Boltzmann operator[37] for the collisions and the GENE uses realistic geometry by using an EFIT file to calculate the magnetic equilibrium. All GENE simulations were made electromagnetically.

The list of simulations is presented in Table I. Although all simulations have an experimental discharge as the base for its parameters, some might be different. Hence, some discharge numbers are recurrent in the table. There are two simulations from AUG, three from DIII-D, and twelve from JET. The JET simulations include three hydrogen plasmas, and the majority have deuterium as main ion species. Only the three DIII-D simulations include an impurity species, carbon, and the others are simulated as pure plasmas. The simulations have been performed with parameters taken from radial position between 0.5 and 0.8, and the ITG mode is the dominant instability for the majority of the discharges.

In this work, we benchmark new EDWM against this particular set of GENE simulations and concerns might be raised that the new version of EDWM only is proficient toward discharges similar to those presented in Table I. However, we have a representative set of discharges for today's experimental devices. The dataset includes L- and H-mode, discharges from three different machines, hydrogen and deuterium discharges, and the data are taken at positions where the turbulent transport dominates. Furthermore, the core functionality of EDWM is unaltered and the eigenvalue solver maintains its integrity with respect to the underlying equations, Eq. (2).

TABLE I. Parameters for the 17 GENE simulations used to benchmark EDWM. All simulations have an experimental discharge as the base for its parameters, but some parameters might have been changed. This is the reason that some of the discharge numbers are recurrent.

Discharge	Machine	ρ_t	Ion	$n_e\,(10^{19}/\mathrm{m}^3)$	$T_e\,(\mathrm{keV})$	$T_i\,(\mathrm{keV})$	a/L_{n_e}	a/L_{T_e}	a/L_{T_i}	q	$\hat{s}$
35552	AUG	0.5	D	10.6	1.22	1.06	0.02	3.36	1.11	1.30	0.65
36143	AUG	0.6	D	5.71	1.63	1.39	0.42	1.48	1.34	1.35	0.85
79811	JET	0.6	D	1.58	1.45	1.43	0.91	2.42	2.33	2.55	0.93
79814	JET	0.6	D	1.47	0.71	0.71	0	2.93	2.93	2.36	1.25
87424	JET	0.6	D	4.70	1.70	1.70	0.10	2.15	2.15	1.95	0.86
87425	JET	0.6	D	4.90	0.80	0.80	0.26	2.22	2.22	1.95	0.92
87496	JET	0.5	D	4.13	2.03	2.03	0.76	2.02	2.02	1.66	0.53
87496	JET	0.5	H	4.13	2.03	2.03	0.76	2.02	2.02	1.66	0.53
90403	JET	0.6	D	3.45	1.68	1.68	0.83	2.51	2.51	1.92	0.63
91526	JET	0.6	D	3.65	1.37	1.37	1.14	2.12	2.12	1.50	0.68
91544	JET	0.5	D	2.58	1.69	1.69	0.89	1.85	1.85	1.59	0.50
91544	JET	0.5	H	2.58	1.69	1.69	0.89	1.85	1.85	1.59	0.50
91544	JET	0.8	D	2.00	0.88	0.88	0.88	2.58	2.57	2.46	1.62
91544	JET	0.8	H	2.00	0.88	0.88	0.88	2.58	2.57	2.46	1.62
165303	DIII-D	0.6	D	3.86	1.98	1.67	0.67	2.55	1.24	2.63	1.51
165320	DIII-D	0.6	D	4.03	0.69	0.96	0	2.84	1.88	2.32	1.40
165325	DIII-D	0.6	D	4.51	1.06	0.99	0.54	2.73	1.38	2.22	1.32

B. GYRO database

The GYRO database was created by over 320 non-linear simulations using the gyrokinetic code GYRO[38–41] and is currently accessible here.[23] Two different types of parameters sets have been studied in the GYRO database, GA standard case, and TEM1. Both cases have been simulated assuming only electrostatic perturbations and without collisions.

The GA standard case is meant to simulate a typical ITG-dominated plasma and its parameters are as follows:

R/a = 3.0	r/a = 0.5	q = 2
$\hat{s} = 1.0$	$\beta = 0$	$\alpha = 0$
$a/L_n = 1.0$	$a/L_T = 3.0$	$T_i/T_e = 1.0$

The TEM1 case is meant to mimic a plasma with mixed ITG and TEM instabilities. Its parameters are as follows:

R/a = 3.0	r/a = 0.5	q = 2
$\hat{s} = 1.0$	$\beta = 0$	$\alpha = 0$
$a/L_n = 2.0$	$a/L_T = 2.0$	$T_i/T_e = 1.0$

C. JET collisionality scans

The last set of data used for the benchmarking with EDWM is four JET collisionality scans. These four collisionality scans consist of three discharges each where all major dimensionless parameters have been kept fixed, such as q, ρ^*, β, and $\tau = T_i/T_e$. The four collisionality scans represent four different plasma regimes, H-mode, L-mode, hydrogen, and high β H-mode. The discharges in question are as follows: 79811, 79815, and 79814 for the L-mode; 87424, 87420, and 87425 for the H-mode; 90403, 90409, and 90411 for the high β H-mode. Finally, 91526, 91530, and 91524 for the hydrogen collisionality scan. There are some overlaps of these discharges with the ones in the GENE simulations, in Table I. For a more thorough presentation of the collisionality scan discharges, see Ref. 42. Fluxes from the collisionality scans have been used to validate the fluxes from the new version of EDWM.

IV. UPDATED VERSION OF EDWM

In this section, we present and discuss the new version of EDWM. The aspects, which have been updated, are as follows: a new spectral filter, adjustment of the collision operator, correction of the discrepancy with the electron heat flux, adjusting the dependency on the safety factor, and finally a new normalization of the flux level.

A. Filter

EDWM calculates the turbulent transport at ion scales and has previously used five poloidal wavenumbers between $k\rho_{s,H}$ 0.1 and 0.5 as a default. For the new version, we expanded to 11 poloidal wavenumber as to properly accommodate the new filter presented in Sec. IV A 1. To have the correct level of flux at all poloidal wavenumbers is crucial because different instabilities appear at different scales. This is especially important for the particle channel, as the major part of the outward diffusion and inward pinch might be located at different scales.[43] Hence, an erroneous filter may quench one and not the other, leading to an incorrect flux. To achieve this, we introduce a new filter for the new version of EDWM. The need for it is easiest explained by looking at the $k\rho_s$ dependency of the electrostatic potential at low $k\rho_s$, as presented in Eq. (5)

$$\hat{\phi} = \frac{\gamma}{k_x k_y} \frac{1}{\rho_s c_s}. \tag{10}$$

EDWM uses the assumption that the radial and poloidal wavelength are of the same magnitude, that is, $k_x \approx k_y$. The growth rates for the ITG mode at low k_y have a linear dependency; $\gamma \propto k_y$.[26] Hence, we get a dependency for the electrostatic potential as $\hat{\phi} \propto k_y^{-1}$. As the potential is directly connected to the saturation level, this causes large fluxes at low k_y. An example of this is displayed in Fig. 1, which shows the electron heat flux for a simulation with the original EDWM. The high level of flux at low k_y is not physical and is not seen in gyrokinetic non-linear simulations due to Landau damping and/or zonal flows.

The shortcoming of the previous model is due to the assumption of isotropic turbulence in the radial and poloidal directions. It has been shown[10] that the poloidal wavenumber is independent of the radial wavelength for low values of k_y. Hence, the electrostatic potential will have a very weak dependency on the poloidal wavenumber for low values. In Sec. IV A 1, a poloidal wavenumber filter will be introduced which counters this erroneous behavior.

1. Implementation of filter

As presented in Sec. II A, we have introduced a filter for the electrostatic potential dependency of the poloidal wavenumber. However, a filter in EDWM is not a new feature, the Casati filer[44] has been part of EDWM for years, and it has had some success especially for ITER simulations; however, this filter was developed for QuaLiKiz and

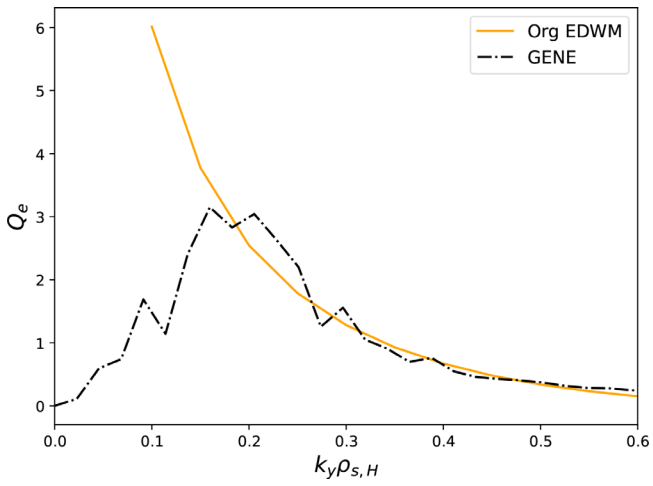

FIG. 1. Electron heat flux for the JET discharge 79811 at $\rho_t = 0.6$ per poloidal wavenumber for the original EDWM model and GENE. The model overestimates the contribution from the very low wavenumbers compared to gyrokinetic simulations.

consequently not optimized for EDWM. We introduce the function $f(k_y)$, which contains all poloidal wavenumber dependency for the electrostatic potential

$$|\hat{\phi}|^2 = \frac{4\gamma_a^2}{\omega_{Dea} R^2 k_a^2} f^2(k_y). \quad (11)$$

Here, "a" denotes the value of the parameters at the characteristic length scale and introduces as k_a, which was discussed in Sec. II A. In order to achieve a proper expression for the electrostatic potential, three things need to be determined:

- The characteristic length k_a
- The spectral shape for k_y smaller than k_a
- The spectral shape for k_y larger than k_a

The characteristic length is the typical length scale for the turbulent transport where we have the highest transport. It has previously been suggested that the maximum of the growth rate of the most unstable mode at ion scale describes the typical length scale.[7] More recent work[45] indicates that the zonal flow velocity dominates the saturation mechanism for the turbulent transport in plasmas. The length scale of the zonal flow velocity is determined by maximum value for γ/k_y. We determine which one describes the correct characteristic by comparing at what poloidal wavenumber the heat and particle flux has their maximum for the 17 GENE simulation in Table I. If the maxima for our two options are far from the GENE simulation maxima, it is a clear indication that it does not dominate the saturation mechanism, and therefore does not determine the characteristic length scale. We calculated the average absolute difference in the poloidal wavenumber for the options against the GENE results, and the choice of the zonal flow as the characteristic length scale was significant better than a filter centered at the maximum growth rate at ion scales. For the growth rate as characteristic length scale, the average absolute distance with the maximum of the fluxes from the GENE simulations over the 51 transport channels (17 discharges, particle, and two heat) was 0.26 $k_y\rho_{s,H}$. The spatial scale of the maximum growth rate was repeatedly too small compared to the GENE results, agreeing with previous work. Using the aforementioned zonal flow velocity's length scale as the characteristic scale gave an average separation of 0.08 $k_y\rho_s$ to the position of the maximum flux from the GENE simulations. Hence, in the new version of EDWM the correlation length is chosen to be at the maximum for γ/k_y corresponding to the saturation mechanism of the zonal flow.

For k_y lower than $k_{a,}$ the choice for $f(k_y)$ was taken so that fluxes have the correct dependency for the ITG-mode turbulence when using the low k_y expansion, discussed in Sec. IV A. This corresponds to a filter of $f = \frac{\gamma}{\gamma_a}\frac{k_a}{k_y}$.

For k_y higher than $k_{a,}$ the choice most suited was $f = \frac{\gamma}{\gamma_a}\frac{k_a^{5/2}}{k_y^{5/2}}$. The complete filter

$$f(k_y) = \frac{\gamma}{\gamma_a}\frac{k_a}{k_y} \quad for \quad 0 - k_a = \frac{\gamma}{\gamma_a}\frac{k_a^{5/2}}{k_y^{5/2}} \; for \; k_a - .$$
$$= \frac{\gamma}{\gamma_a}\frac{k_a^{5/2}}{k_y^{5/2}} \quad for \quad k_a - . \quad (12)$$

An example of the comparison of the fluxes per k_y between the new version of EDWM with the filter and GENE is shown in Fig. 2 for the JET discharge 91544, at ρ_t 0.8 with deuterium as ion species. In (a), the ion heat flux is displayed, in (b) the electron heat flux, and in

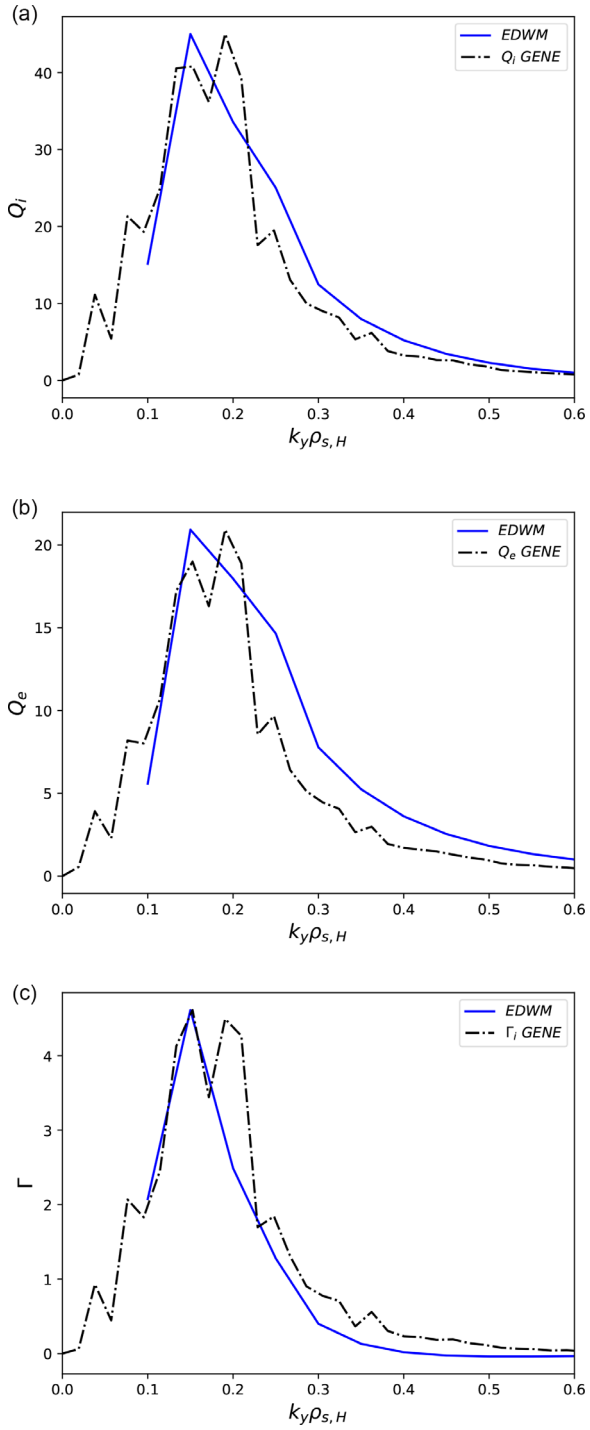

FIG. 2. Comparison of fluxes of ion energy (a), electron energy (b), and particle flux (c) between a non-linear GENE simulation and new EDWM for JET discharge 91544 at ρ_t at 0.8 with deuterium as ion species. EDWM captures the spectral shape for all transport channels in a satisfactory way. The magnitude of the EDWM fluxes has been normalized with maximum level from the GENE simulations.

(c) the electron particle flux. The level of the EDWM fluxes is normalized to the same maximum level as the GENE fluxes to make the comparison between the spectral shapes as clear as possible. The saturation level of EDWM is adjusted and discussed in Sec. IV E. The choice of the zonal flow length scale as the characteristic length works well for this simulation as the peak for EDWM coincide with GENE counterparts and captures the spectral shape from the GENE simulations.

In order to get a more quantified assessment of the filter's performance, we have calculated two figures of merit: mean absolute error (MAE) for the position of the highest flux per k_y, that is, the peak, and the average spectral width of fluxes. The MAE for the peak position between the GENE and the new EDWM simulations is 0.08, which may be compared with the average peak for the GENE simulations, which is at $k_y = 0.25$. The width of the peak was determined by the positions where the fluxes had been lowered to 1/e of the peak value. The new EDWM simulations have a width of 0.19, compared to the GENE results, which have a width of 0.23.

B. Collisionality factor

As EDWM is a fluid model, the adaption of a proper collision operator is not obvious. The EDWM collision operator is described in detail in Ref. 46, and it works well at low and high collisionalities; however, at intermediate collisionality, it is not as proficient. We aim to update the EDWM collision operator by benchmarking it for the GA standard case against the gyrofluid model TGLF and linear simulations with GENE. This is done by investigating the zero flux peaking factor for the discharge, and it is determined by the particle flux, which has an outward diffusive part and a convective part, which is usually inward. The zero flux peaking factor is the normalized density gradient, which causes the turbulent particle transport to have zero flux, and it is the normalized gradient a plasma has in steady state if it does not have any internal sources. As it is sensitive to the collisionality, it is suitable for the collision operator tuning.[25] This is done by scaling the collision frequency with a factor α.

We have calculated the zero flux peaking factor at different fractions (0%–100%) of the GA standard case collision frequency and compare the results in Fig. 3. TGLF and linear GENE with $k_y\rho_{s,H} = 0.3$ show a similar dependence on the collisionality with a small offset. Original EDWM is in agreement in the collisionless limit; however, at larger fractions, the result diverges from TGLF and GENE. New EDWM solves this by multiplying the collision frequency with a factor of $\alpha = 1/3$. The result for new EDWM is the orange line in Fig. 3, and it is well matched with the other codes.

C. Electron heat flux

Original EDWM yields too low electron heat flux compared to its ionic counterpart. In predictive simulations, this might cause additional problems as too low electron heat flux lead to high electron temperature and a large equipartition term between electrons and ions. Consequently, the original EDWM overestimates the ion temperature as well. In order to investigate this problem, we compared the fluxes provided by EDWM with the fluxes from the GENE simulations described in Table I. We calculated the fraction between the ion and electron heat flux, particle flux and ion heat flux, and finally between particle flux and electron heat flux. The average ratio over all simulations for GENE and original EDWM is presented in Table II. The table

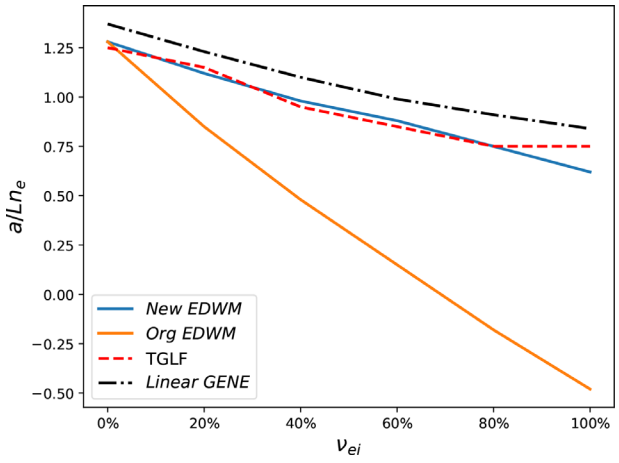

FIG. 3. Zero flux peaking factor, the normalized density gradient where the turbulent transport yield no particle flux, for the GA standard case calculated with TGLF, linear GENE, original EDWM, and new EDWM.

confirms that the original EDWM has a too low electron heat flux as it overestimates the Q_i/Q_e- and Γ_e/Q_e-fraction compared to the GENE simulations. Hence, a multiplication factor of 2.88, the average value for the two fractions, has been included for the electron heat flux in the new EDWM. The fraction for the particle flux and ion heat flux is comparable between GENE and original EDWM and will not be updated.

Results for the new version of EDWM, with the added factor, compared with the GENE fractions are presented in Fig. 4, and EDWM performs relatively well on average. However, there are some discrepancies, which the current reduced model cannot resolve. In Fig. 4(a), we displayed the Q_i/Q_e-fraction. Figure 4(b) displays the unaltered fraction of Γ_e/Q_i for EDWM and it is comparable with the GENE counterpart. For the Γ_e/Q_e-fraction in Fig. 4(c), the new version of EDWM performs good in general. However, for two of the JET discharges, new EDWM overpredicts the ratio significantly.

D. Safety factor dependency

Original EDWMs' response to the safety factor has been updated in the new version by comparing with safety factor scans done with the gyrokinetic code GYRO.[41] Results show that a stronger dependency is needed which will lead to a larger transport in the outer regions of typical plasma discharges. The further correction is needed due to kinetic effects, which are not included in the fluid models.[47]

TABLE II. Average fraction for Q_i/Q_e, Γ_e/Q_i, and Γ_e/Q_e for all 17 GENE simulations and identical original EDWM simulations. The last row displays the fraction of the EDWM and GENE fraction. The results clearly show that the original EDWM has too low heat flux.

Model	Q_i/Q_e	Γ_e/Q_i	Γ_e/Q_e
GENE	1.77	0.08	0.15
EDWM	4.53	0.09	0.49
EDWM/GENE	2.56	1.06	3.18

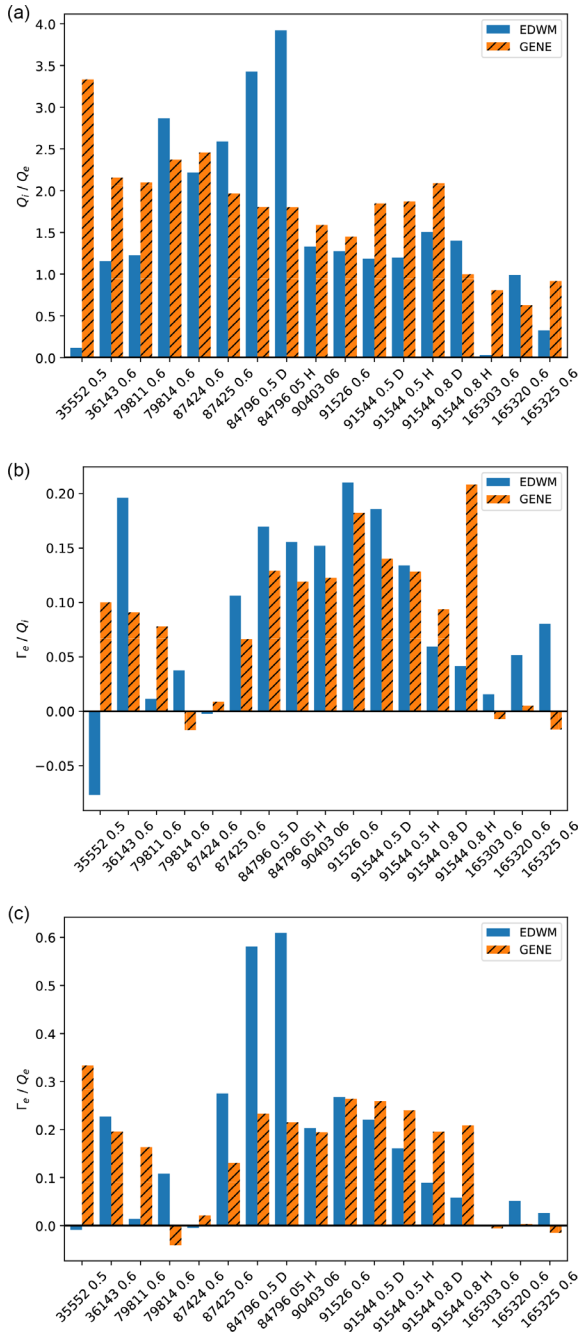

FIG. 4. Fraction for Q_i/Q_e, Γ_e/Q_i, and Γ_e/Q_e for all 17 GENE simulations and identical new EDWM simulations. The new EDWM generally has a good value for the ratio compared to GENE.

The safety factor effects the transport in EDWM in several ways including electromagnetic effects. We have compared our simulations with EDWM with safety factor scans, which have been performed with the GA standard case, with $\hat{s} = 1$ and $\hat{s} = 1.5$, and TEM1 case, both which are described in Sec. III B. It is important to mention that the simulations of the safety factor scans made in the GYRO database have been performed for the electrostatic case. Our EDWM simulations have been performed in the electrostatic case as well to capture the same physics. Therefore, the dependence on the safety factor is not unrelated to electromagnetic effects.

TABLE III. The best power fit for the fluxes for the GYRO safety factor scans. The table displays the power.

Discharge	GA $\hat{s} = 1$	GA $\hat{s} = 1.5$	TEM1
Q_i	0.85	1.10	0.67
Γ_e	−0.01	0.37	0.64
Q_e	0.90	1.32	0.91

We display the safety factor power dependence from the GA database in Table III. The heat flux shows a stronger dependence of the safety factor than the particle fluxes and the strongest effect is seen for the GA standard cases. The result of the EDWM scans displayed that original EDWM has a weak dependence of the safety factor, and the power factor dependence is close to 0. It is clear that the GYRO simulation has a much stronger dependency which EDWM does not capture. The heat fluxes also have a larger discrepancy between GYRO and EDWM. Hence, we will add a different coefficient for the particle and heat fluxes in the implementation in EDWM. The average different dependencies between the EDWM result and GYRO database are as follows: particle flux, 0.09, and heat flux, 0.77. These two coefficients have been implemented as power law corrections for the safety factor on the fluxes which EDWM provides.

The new version of EDWM is shown for the heat fluxes for the GA standard case with $\hat{s} = 1$ in Fig. 5.

E. Normalize the fluxes

The last update we present in this paper is the normalization level for the fluxes. As the original EDWM normalization level was with 5 poloidal wavenumbers instead of 11 and without the updates presented, the level needs to be adjusted. We have performed the normalization comparing EDWM fluxes with those from GENE simulations. The comparison has been made with the parameters displayed in Table I, and the average fraction of the fluxes obtained from EDWM and GENE for all simulations has been calculated. The results for the EDWM and GENE fractions are presented in Table IV. We can notice that the ratio for both heat channels is similar, which is as expected as the new version of EDWMs heat transport was adjusted according to the GENE data in Sec. IV C. EDWM overpredicts all fluxes, which is mainly due to the increase from 5 to 11 poloidal wavenumber. The average difference for the three channels is 4.17, indicating that the values in EDWM should be lowered with a factor of that magnitude to get an appropriate agreement with GENE results. This factor has been added to the new version of EDWM.

F. Validation of the flux levels

In order to validate the new version of EDWM, we have compared it against experimental fluxes from the collisionality scan discharges presented in Sec. III C. The experimental fluxes from the collisionality scans discharges are taken at the quasi-steady state, where

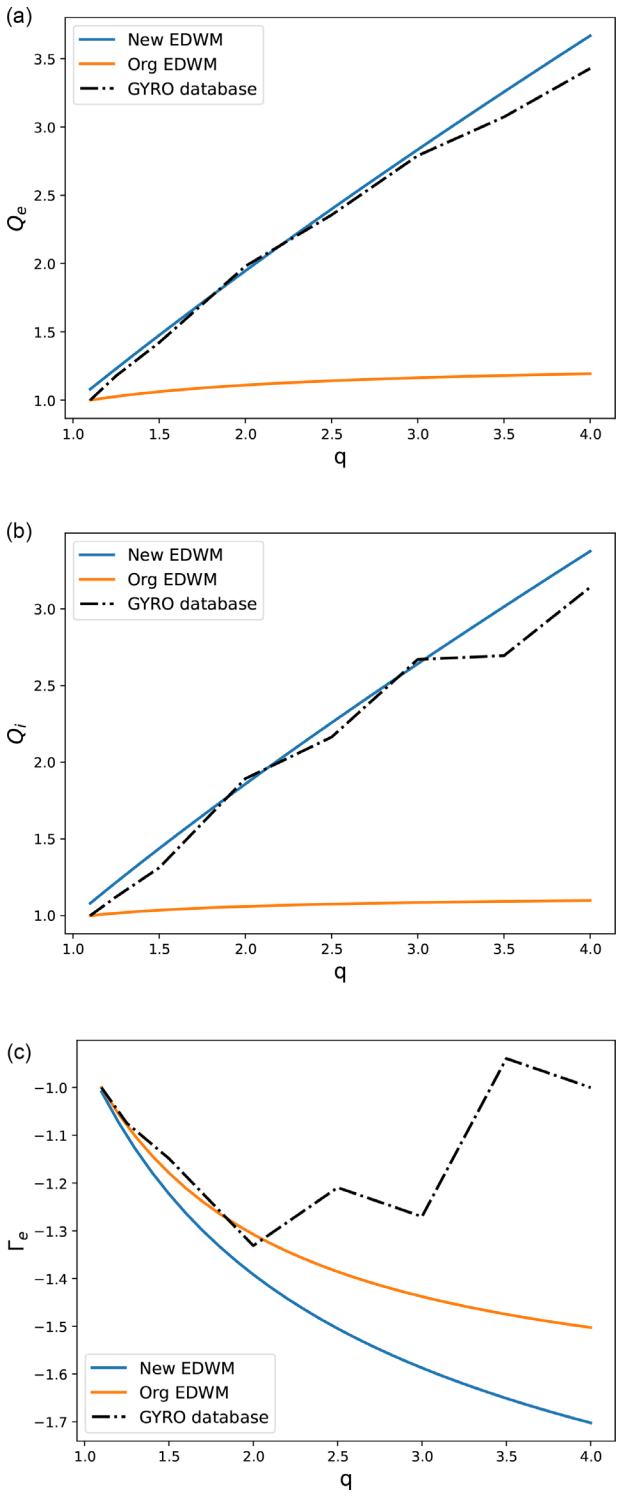

FIG. 5. Safety factor scan for GA standard case with $\hat{s} = 1$ compared with original EDWM and new EDWM for electron heat flux (a), ion heat flux (b), and electron particle flux (c). All fluxes are normalized q = 1.1 to emphasize the safety factor dependency.

TABLE IV. The average ratio for the fluxes of the new EDWM divided with GENE. The results indicate that EDWM needs to lower its fluxes with an average factor of 4.17.

Flux	EDWM/GENE
Q_i	3.60
Γ_e	4.85
Q_e	4.06

TABLE V. The average fluxes from the new EDWM divided with experimental measured fluxes. The new version of EDWM has a similar flux for the ion heat flux and electron particle flux. However, it gives a too high election heat flux.

Flux	EDWM/exp
Q_i	0.72
Γ_e	1.29
Q_e	0.52

the internal sources (NBI-beams, RF-heating) match the outward fluxes. The internal sources have been calculated using the integrated modeling tool JINTRAC and put equal as the experimental fluxes. We have performed the comparison at four radial positions for each discharge, and we have compared the electron particle flux, electron heat flux, and the ion heat flux. The four radial positions used in the comparison are ρ_t: 0.4, 0.5, 0.6, 0.7, where ρ_t is in the normalized flux label. In total, 144 fluxes were compared and the average fraction between calculated and experimental fluxes is displayed in Table V. The results show that fluxes calculated by EDWM are similar to the experimental for the ion heat flux and electron particle flux. However, the new version of EDWM gives too low electron heat flux for these discharges, approximately a factor of 2. This is an acceptable agreement as the stiffness of the turbulent transport makes the transport sensitive the driving gradient, that is, yields similar profiles.

V. SUMMARY AND OUTLOOK

In this work, we have presented the latest updates and calibrations of the quasi-linear fluid model EDWM. A new saturation model has been constructed, based on and verified against non-linear gyrokinetic simulations. The model calculates a saturation level at the correlation length and uses a spectral filter for the poloidal wavenumber dependency. The shape of the filter has been fitted toward poloidal wavenumber dependency for the electrostatic potential from nonlinear gyrokinetic simulations. The filter solves a previous shortcoming of EDWM: its tendency to generate a too large flux for low wavenumbers. The collision operator has been calibrated to fit the zero flux peaking factor and the normalized density gradient, which gives zero flux for the turbulent transport, for the GA standard case. The benchmarking showed that the original EDWM collision operator was too strong and a correction factor of 1/3 was applied to the collision frequency for the new version of EDWM. Original EDWM has previously calculated a too small electron heat flux, and by calibrating the ratio of the transport channels, the new version of EDWM gives a larger electron heat flux. EDWMs' response to the safety factor has also been improved by comparing with safety factor scans done with

the gyrokinetic code GYRO.[41] The result indicates that a further correction is needed due to kinetic effects, which are not included in the fluid models. These effects are included by introducing power law correction to the transport channels as discussed in Sec. IV D. The updated q-scaling in the new version of EDWM will lead to a larger predicted transport in the outer regions of the plasma. The saturation level was finally calibrated by benchmarking against non-linear gyrokinetic GENE simulations, required as the new version of EDWM uses 11 poloidal wavenumbers, instead of 5 and the updates effects the fluxes. A common saturation level was determined for all transport channels.

The saturation level has been verified against experimental measurements for fluxes at four radial positions for 12 discharges, which have been achieved by analyzing the profiles at quasi-steady state. The new version of EDWM performed well for ion heat flux and particle flux. However, some discrepancy was found for the electron heat flux, and the new EDWM gave too large electron heat flux.

Future work involves using the new version of EDWM as a part of an integrated model. It is important to perform predictive simulations to verify that the new EDWM captures the complex interplay between different properties in the plasma in a self-consistent treatment. EDWM was designed to handle different isotopes, and as new experimental result from the latest JET DTE2-campaign emerges, it is prudent to investigate the isotope effect of the model. However, some steps have already been taken, as the new filter is adaptive to the shift in the poloidal wavenumber, which occurs for different isotopes.

ACKNOWLEDGMENTS

The authors would like to thank Lars-Göran Eriksson for fruitful discussions.

This work has been carried out within the framework of the EUROfusion Consortium, funded by the European Union via the Euratom Research and Training Programme (Grant Agreement No 101052200—EUROfusion). Views and opinions expressed are however those of the author(s) only and do not necessarily reflect those of the European Union or the European Commission. Neither the European Union nor the European Commission can be held responsible for them.

The simulations were performed on resources provided by the Swedish National Infrastructure for Computing (SNIC) at PDC-HPC and the MARCONI (CINECA, Bologna, Italy) supercomputer systems.

AUTHOR DECLARATIONS

Conflict of Interest

The authors have no conflicts to disclose.

Author Contributions

Emil Fransson: Conceptualization (equal); Data curation (lead); Formal analysis (lead); Investigation (lead); Methodology (equal); Software (equal); Validation (lead); Visualization (lead); Writing – original draft (lead); Writing – review & editing (equal). **Hans Nordman:** Conceptualization (lead); Investigation (equal); Methodology (equal); Writing – review & editing (lead). **Pär Strand:** Conceptualization (equal); Funding acquisition (lead); Resources (equal); Software (equal); Supervision (lead); Writing – review & editing (supporting).

DATA AVAILABILITY

The data that support the findings of this study are available from the corresponding author upon reasonable request.

REFERENCES

[1]D. Coster, V. Basiuk, G. Pereverzev, D. Kalupin, R. Zagórski, R. Stankiewicz, P. Huynh, F. Imbeaux, and Members of the Task Force on Integrated Tokamak Modelling, "The European transport solver," IEEE Trans. Plasma Sci. **38**, 2085–2092 (2010).

[2]D. Kalupin, I. Ivanova-Stanik, I. Voitsekhovitch, J. Ferreira, D. Coster, L. L. Alves, Th. Aniel, J. F. Artaud, V. Basiuk, J. P. S. Bizarro *et al.*, "Numerical analysis of JET discharges with the European transport simulator," Nucl. Fusion **53**, 123007 (2013).

[3]G. V. Pereverzev and P. N. Yushmanov, "ASTRA—Automated system for transport analysis," IPP-Report No. IPP 5/98 (Max-Planck-Institut Für Plasmaphysik, 2002).

[4]G. Cennachi and A. Taroni, JETTO: Technical Report No. JET-IR (88) 03 (JET Reports, 1988).

[5]C. Bourdelle, X. Garbet, F. Imbeaux, A. Casati, N. Dubuit, R. Guirlet, and T. Parisot, "A new gyrokinetic quasilinear transport model applied to particle transport in tokamak plasmas," Phys. Plasmas **14**, 112501 (2007).

[6]G. M. Staebler, J. E. Kinsey, and R. E. Waltz, "Gyro-Landau fluid equations for trapped and passing particles," Phys. Plasmas **12**, 102508 (2005).

[7]J. Weiland, *Collective Modes in Inhomogeneous Plasma* (Institute of Physics Building, 2000).

[8]P. Strand, G. Bateman, A. Eriksson, W. A. Houlberg, A. H. Kritz, H. Nordman, and J. Weiland, "Comparisons of anomalous and neoclassical contributions to core particle transport in tokamak discharges," in *Proceedings of the 31st EPS Conference on Plasma Physics* (2004), Paper No. 28G P-5.187.

[9]C. Bourdelle, J. Citrin, B. Baiocchi, A. Casati, P. Cottier, X. Garbet, F. Imbeaux, and JET Contributors, "Core turbulent transport in tokamak plasmas: Bridging theory and experiment with QuaLiKiz," Plasma Phys. Controlled Fusion **58**, 014036 (2016).

[10]G. M. Staebler, E. A. Belli, J. Candy, J. E. Kinsey, H. Dudding, and B. Patel, "Verification of a quasi-linear model for gyrokinetic turbulent transport," Nucl. Fusion **61**, 116007 (2021).

[11]J. Garcia, N. Hayashi, B. Baiocchi, G. Giruzzi, M. Honda, S. Ide, P. Maget, E. Narita, M. Schneider, H. Urano, JT-60U Team, and JET EFDA Contributors and EU-ITM ITER Scenario Modelling Group, "Physics comparison and modelling of the JET and JT-60U core and edge: towards JT-60SA predictions," Nucl. Fusion **54**, 093010 (2014).

[12]F. J. Casson, H. Patten, C. Bourdelle, S. Breton, J. Citrin, F. Koechl, M. Sertoli, C. Angioni, Y. Baranov, R. Bilato *et al.*, "Predictive multi-channel flux-driven modelling to optimise ICRH tungsten control and fusion performance in JET," Nucl. Fusion **60**, 066029 (2020).

[13]G. Tardini, C. Angioni, C. K. Kiefer, T. Luda, N. Bonanomi, M. Dunne, E. Fable, F. Ryter, and ASDEX Upgrade Team, "Towards fully-predictive transport modelling in ASDEX Upgrade H-modes," Nucl. Fusion **61**, 126045 (2021).

[14]T. Luda, C. Angioni, M. G. Dunne, E. Fable, A. Kallenbach, N. Bonanomi, P. A. Schneider, M. Siccinio, G. Tardini, and ASDEX Upgrade Team and EUROfusion MST1 Team, "Integrated modeling of ASDEX Upgrade plasmas combining core, pedestal and scrape-off layer physics," Nucl. Fusion **60**, 036023 (2020).

[15]M. Marin, J. Citrin, C. Bourdelle, Y. Camenen, F. J. Casson, A. Ho, F. Koechl, M. Maslov, and JET Contributors, "First-principles-based multiple-isotope particle transport modelling at JET," Nucl. Fusion **60**, 046007 (2020).

[16]G. M. Staebler, M. Knolker, P. Snyder, C. Angioni, E. Fable, T. Luda, C. Bourdelle, J. Garcia, J. Citrin, M. Marin *et al.*, "Advances in prediction of tokamak experiments with theory-based models," Nucl. Fusion **62**, 042005 (2022).

[17]O. Meneghini, P. B. Snyder, S. P. Smith, J. Candy, G. M. Staebler, E. A. Belli, L. L. Lao, J. M. Park, D. L. Green, W. Elwasif, B. A. Grierson, and C. Holland,

"Integrated fusion simulation with self-consistent core-pedestal coupling," Phys. Plasmas **23**, 042507 (2016).
[18]J. M. Park, J. R. Ferron, C. T. Holcomb, R. J. Buttery, W. M. Solomon, D. B. Batchelor, W. Elwasif, D. L. Green, K. Kim, O. Meneghini, M. Murakami, and P. B. Snyder, "Integrated modeling of high β_N steady state scenario on DIII-D," Phys. Plasmas **25**, 012506 (2018).
[19]O. Meneghini, G. Snoep, B. C. Lyons, J. McClenaghan, C. S. Imai, B. Grierson, S. P. Smith, G. M. Staebler, P. B. Snyder, J. Candy *et al.*, "Neural-network accelerated coupled core-pedestal simulations with self-consistent transport of impurities and compatible with ITER IMAS," Nucl. Fusion **61**, 026006 (2021).
[20]C. Angioni, T. Gamot, G. Tardini, E. Fable, T. Luda, N. Bonanomi, C. K. Kiefer, G. M. Staebler, ASDEX Upgrade Team, and EUROfusion MST1 Team, "Confinement properties of L-mode plasmas in ASDEX Upgrade and full-radius predictions of the TGLF transport model," Nucl. Fusion **62**, 066015 (2022).
[21]G. M. Staebler, J. Candy, E. A. Belli, J. E. Kinsey, N. Bonanomi, and B. Patel, "Geometry dependence of the fluctuation intensity in gyrokinetic turbulence," Plasma Phys. Controlled Fusion **63**, 015013 (2021).
[22]F. Jenko and W. Dorland, "Nonlinear electromagnetic gyrokinetic simulations of tokamak plasmas," Plasma Phys. Controlled Fusion **43**, A141–A150 (2001).
[23]See https://gafusion.github.io/doc/_downloads/3881d4fcf0de4ae62c476c508fc379e1/gyro-database.pdf for the GYRO database.
[24]W. Horton, *Turbulent Transport in Magnetized Plasmas* (World Scientific Publishing Company, 2012).
[25]C. Angioni, A. G. Peeters, G. V. Pereverzev, F. Ryter, G. Tardini, and ASDEX Upgrade Team, "Density peaking, anomalous pinch, and collisionality in tokamak plasmas," Phys. Rev. Lett. **90**, 205003 (2003).
[26]H. Nordman and J. Weiland, "Transport due to toroidal η_i mode turbulence in tokamaks," Nucl. Fusion **29**, 251 (1989).
[27]H. Nordman, J. Weiland, and A. Jarmén, "Simulation of toroidal drift mode turbulence driven by temperature gradients and electron trapping," Nucl. Fusion **30**, 983 (1990).
[28]M. Fröjdh, M. Liljeström, and H. Nordman, "Impurity effects on η_i mode stability and transport," Nucl. Fusion **32**, 419 (1992).
[29]T. S. Hahm and K. Burell, "Flow shear induced fluctuation suppression in finite aspect ratio shaped tokamak plasma," Phys. Plasmas **2**, 1648 (1995).
[30]W. Guttenfelder, J. Candy, S. M. Kaye, W. M. Nevins, E. Wang, R. E. Bell, G. W. Hammett, B. P. LeBlanc, D. R. Mikkelsen, and H. Yuh, "Electromagnetic transport from microtearing mode turbulence," Phys. Rev. Lett. **106**, 155004 (2011).
[31]G. Bateman, A. H. Kritz, J. E. Kinsey, A. J. Redd, and J. Weiland, "Predicting temperature and density profiles in tokamaks," Phys. Plasmas **5**, 1793 (1998).
[32]T. Dannert and F. Jenko, "Gyrokinetic simulation of collisionless trapped-electron mode turbulence," Phys. Plasmas **12**, 072309 (2005).
[33]F. Jenko, T. Dannert, and C. Angioni, "Heat and particle transport in a tokamak: Advances in nonlinear gyrokinetics," Plasma Phys. Controlled Fusion **47**, B195–B206 (2005).
[34]R. Kubo, "The role of zonal flows in the saturation of multi-scale gyrokinetic turbulence," J. Math. Phys. **4**, 174 (1963).
[35]A. Casati, C. Bourdelle, X. Garbet, F. Imbeaux, J. Candy, F. Clairet, G. Dif-Pradalier, G. Falchetto, T. Gerbaud, V. Grandgirard *et al.*, "Validating a quasi-linear transport model versus nonlinear simulations," Nucl. Fusion **49**, 085012 (2009).
[36]J. Citrin, C. Bourdelle, P. Cottier, D. F. Escande, Ö. D. Gürcan, D. R. Hatch, G. M. D. Hogeweij, F. Jenko, and M. J. Pueschel, "Quasilinear transport modelling at low magnetic shear," Phys. Plasmas **19**, 062305 (2012).
[37]F. Merz, "Gyrokinetic simulation of multimode plasma turbulence," Ph.D. thesis (Universitat Munster, 2008).
[38]J. Candy and R. E. Waltz, "Anomalous transport scaling in the DIII-D tokamak matched by supercomputer simulation," Phys. Rev. Lett. **91**, 045001 (2003).
[39]J. Candy and R. E. Waltz, "An Eulerian gyrokinetic-Maxwell solver," J. Comput. Phys. **186**, 545–581 (2003).
[40]J. Candy, R. E. Waltz, and W. Dorland, "The local limit of global gyrokinetic simulations," Phys. Plasmas **11**, L25 (2004).
[41]J. Candy and E. Belli, "GYRO technical guide," General Atomics Technical Report No. GA-A26818, 2010.
[42]T. Tala, H. Nordman, A. Salmi, C. Bourdelle, J. Citrin, A. Czarnecka, F. Eriksson, E. Fransson, C. Giroud, J. Hillesheim *et al.*, "Density peaking in JET—Driven by fuelling or transport?," Nucl. Fusion **59**, 126030 (2019).
[43]C. Angioni, J. Candy, E. Fable, M. Maslov, A. G. Peeters, R. E. Waltz, and H. Weisen, "Particle pinch and collisionality in gyrokinetic simulations of tokamak plasma turbulence," Phys. Plasmas **16**, 060702 (2009).
[44]A. Casati, "A quasi-linear gyrokinetic transport model for tokamak plasmas," Ph.D. thesis (Universite de Provence, France, 2012).
[45]G. M. Staebler, J. Candy, N. T. Howard, and C. Holland, "The role of zonal flows in the saturation of multi-scale gyrokinetic turbulence," Phys. Plasmas **23**, 062518 (2016).
[46]J. Nilsson and J. Weiland, "Fluid model for general collisionality and magnetic curvature," Nucl. Fusion **34**, 803 (1994).
[47]J. E. Kinsey, R. E. Waltz, and J. Candy, "The effect of safety factor and magnetic shear on turbulent transport in nonlinear gyrokinetic simulations," Phys. Plasmas **13**, 022305 (2006).